Evolution of oxide nanoparticles during dynamic plastic deformation of ODS steel

Zhang, Zhenbo; Mishin, Oleg; Tao, Nairong; Pantleon, Wolfgang

Published in:
Risoe International Symposium on Materials Science. Proceedings

Publication date:
2014

Document Version
Early version, also known as pre-print

EVOLUTION OF OXIDE NANOPARTICLES DURING DYNAMIC PLASTIC DEFORMATION OF ODS STEEL

Zhenbo Zhang[*,#], Oleg V. Mishin[*,#], Nairong Tao[**,#], and Wolfgang Pantleon[***,#]

[*] Danish-Chinese Center for Nanometals, Section for Materials Science and Advanced Characterization, Department of Wind Energy, Technical University of Denmark, 4000 Roskilde, Denmark
[**] Institute of Metal Research, Chinese Academy of Science, 110016 Shenyang, China
[***] Section of Materials and Surface Engineering, Department of Mechanical Engineering, Technical University of Denmark, 2800 Kgs. Lyngby, Denmark
[#] Sino-Danish Center for Education and Research

ABSTRACT

The microstructure as well as the deformation behavior of oxide nanoparticles has been analyzed in the ferritic ODS steel PM2000 after compression by dynamic plastic deformation (DPD) to different strains. A dislocation cell structure forms after deformation to a strain of 1.0. DPD to a strain of 2.1 results in nanoscale lamellae with an average lamellar spacing of approximately 70 nm. During DPD oxide nanoparticles, identified as yttrium aluminum perovskite $YAlO_3$, are found to deform differently depending on their size. Whereas particles with a size of less than 15 nm change their shape and aspect ratio, particles coarser than 20 nm remain stable. It is suggested that the small oxide particles in our material are intrinsically easier to be deformed than coarser ones.

1. INTRODUCTION

Oxide-dispersion-strengthened (ODS) steels are promising structural materials for next-generation fission and fusion reactors because of their excellent resistance to both irradiation damage and high-temperature creep (Odette, Alinger and Wirth 2008; Chant and Murty 2010). Since nanoscale oxide dispersoids play a key role in enabling such attractive properties, the particle structure and their stability at high temperatures and in irradiation environments have been studied extensively (Miller, Hoelzer, Kenik and Russell 2005; Hsiung, Fluss, Tumey, Choi, Serruys, Willaime and Kimura 2010; Hirata, Fujita, Wen, Schneibel, Liu and Chen 2011; Ribis and de Carlan 2012). Whereas the thermal behaviour and radiation resistance of oxide particles

in ODS steels have been the topic of many previous studies, very little is known about their response to plastic deformation. The latter is important as processing of ODS steels typically involves plastic deformation, which may not only affect various parameters of the microstructure, but also the morphology and structure of the oxide particles and the oxide-matrix interface. In turn, this can alter the thermal stability and irradiation tolerance of the material. In the present work, the microstructure of ferritic ODS steel PM2000 is investigated in the as-received condition and after dynamic plastic deformation (DPD) (Li, Tao and Lu 2008), with a special focus on the evolution of nanoparticles. To enable a detailed quantitative analysis of nanoparticles, both conventional transmission electron microscopy (TEM) and high resolution TEM are employed in this study.

2. EXPERIMENTAL

A sample of PM2000 (Table 1) with yttria nanodispersoids was received in the form of a hot-extruded rod with a diameter of 13 mm. Cylindrical specimens having a diameter of 6 mm and height of 9 mm were machined with their cylinder axis along the extrusion direction. Compression of the cylinders was carried out by DPD at room temperature with a strain rate of $10^2 – 10^3$ s^{-1}. Samples were investigated after compression by DPD to equivalent strains of 1.0 and 2.1, reached by two and five passes, respectively.

Table 1. Nominal chemical composition (wt. %) of PM2000.

Cr	Al	Ti	Y_2O_3	Fe
20	5.5	0.5	0.5	Bal.

The microstructure of the as-received and DPD samples was first analysed in a JEOL 2000 FX transmission electron microscope. Energy dispersive X-ray (EDX) analysis, high resolution transmission electron microscopy (HRTEM) and scanning transmission electron microscopy (STEM) studies of nanoparticles were carried out using a JEOL 3000F microscope operating at 300 kV.

3. RESULTS

3.1 Initial microstructure. A bright field TEM image (Fig. 1a) shows the microstructure in the longitudinal section of the as-received material. This hot-extruded material is characterized by nearly equiaxed subgrains with a mean size of 1.1 μm and a high dislocation density. A dark field TEM image (Fig. 1b) reveals a high frequency of well dispersed oxide particles in the ferritic matrix. The particle images are circular and their average diameter is 14 nm, which is consistent with the data reported for the same material by Krautwasser, Czyrska-Filemonowicz, Widera and Carsughi (1994). Our HRTEM characterization of the particle structure indicates that these oxide particles can be identified as yttrium aluminum perovskite ($YAlO_3$), which has an orthorhombic structure with lattice parameters of a = 5.330Å, b = 7.375Å and c = 5.180Å. An example HRTEM image of an oxide particle and its corresponding Fast Fourier Transformation (FFT) pattern is shown in Fig. 2. In this case, the incident electron beam is nearly along a zone axis with a low index of $YAlO_3$, and the corresponding FFT is identical to the simulated diffraction patterns of $YAlO_3$ viewing along the ⟨012⟩ orientation.

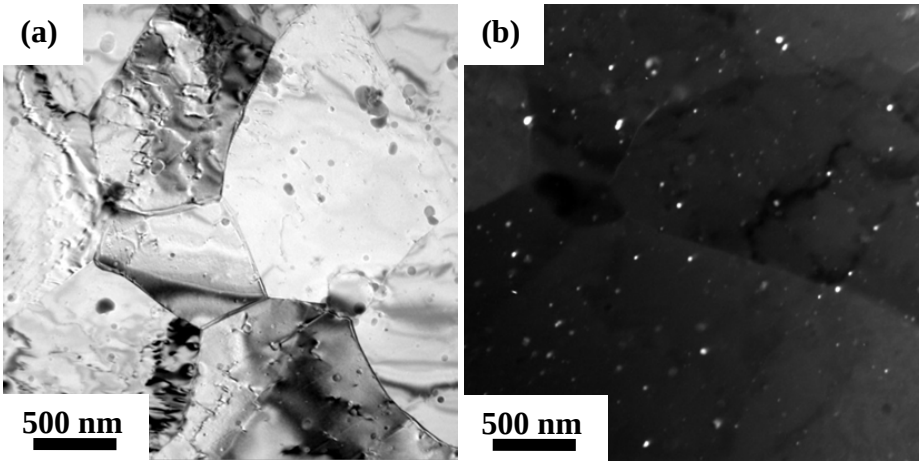

Fig. 1. TEM images from the longitudinal section of the as-received condition of PM2000: (a) a bright field image showing primarily subgrain and dislocation structure. Particles are seen as dark features; and (b) a dark field TEM image (from a different region), where the particles are seen as bright features. The extrusion direction is parallel to the scale bar.

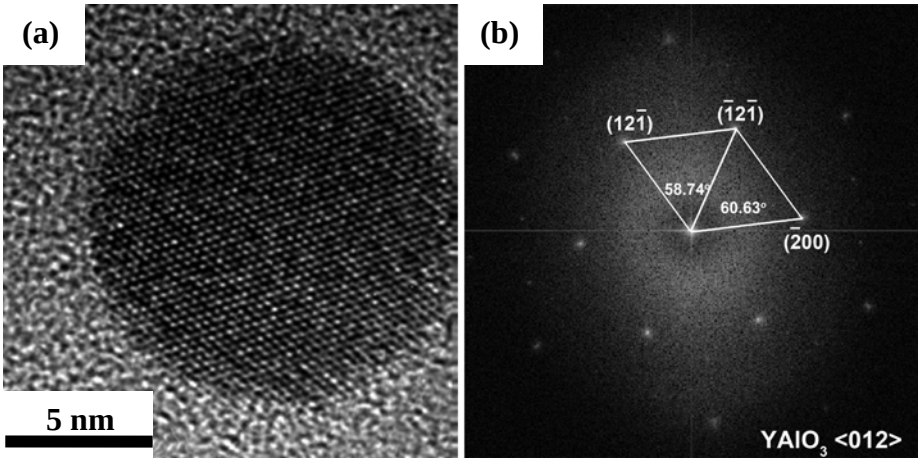

Fig. 2. HRTEM image (a) and corresponding Fast Fourier Transformation (FFT) image (b) of an oxide particle in the as-received condition of PM2000.

3.2 Microstructure after DPD. Bright field TEM images of samples after DPD are shown in Fig. 3. A dislocation cell structure is observed after DPD to a strain of 1.0 (see Fig. 3a). In contrast, a nanoscale lamellar structure with lamellar boundaries nearly perpendicular to the compression direction is developed after deformation to a strain of 2.1 (Fig. 3b). The interlamellar boundary spacing is 70 nm. It is evident that the deformation microstructure contains dark elongated features, which can be seen more clearly in the magnified regions on the right-hand side of Fig. 3a and Fig. 3b. These features are aligned almost perpendicular to the compression axis. A STEM image of the DPD sample is shown in Fig. 4, and an EDX line scanning spectrum provides evidence that these features are enriched in Y and Al, but depleted in Fe and Cr, which suggests that they are oxide nanoparticles, with the shape altered due to compression by DPD from the original spheres to disks. This result indicates that the oxide nanoparticles become plastically deformed during DPD. The disk shape is further verified by observations of particles from a different section that contains the DPD plane (see Fig. 5). It is seen that the disks are not perfectly round in the compression plane, which may be due to anisotropic deformation of individual particles.

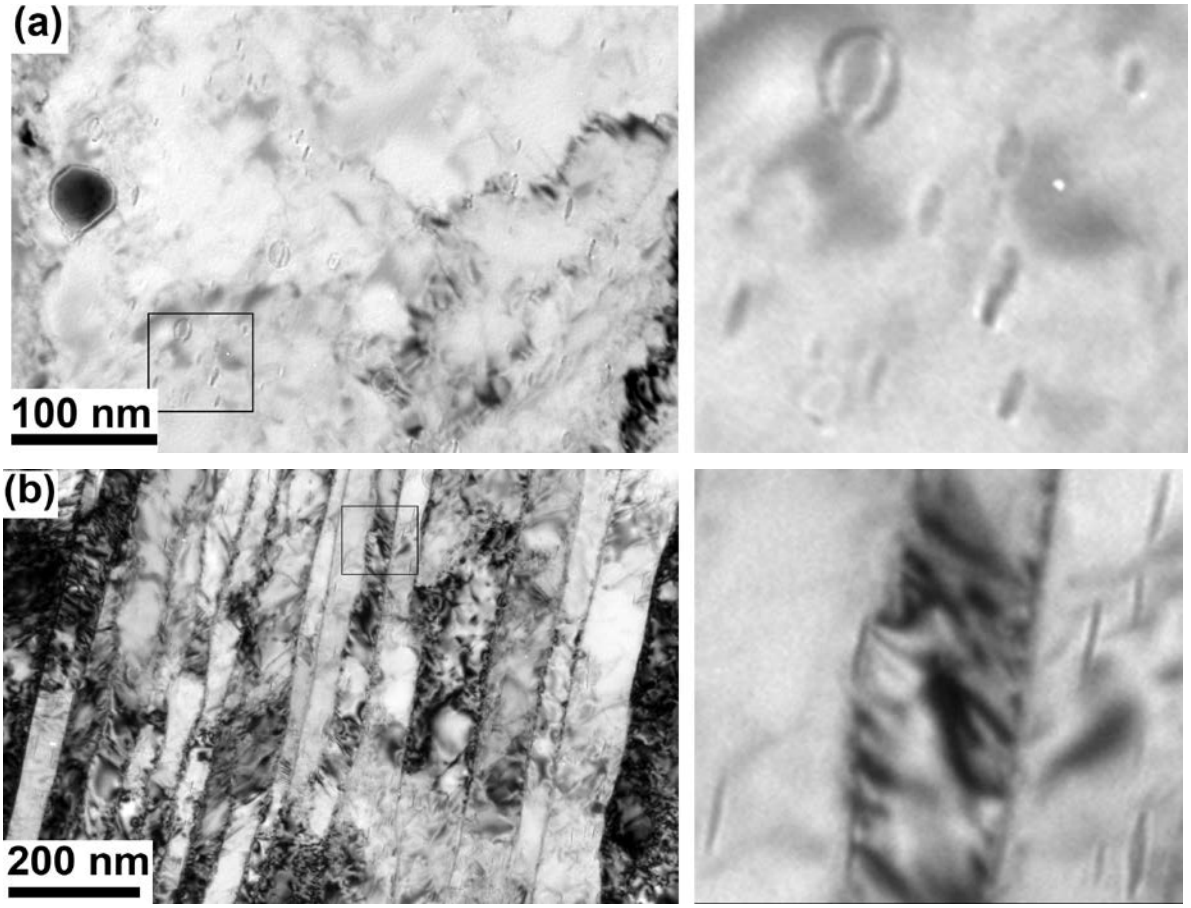

Fig. 3. TEM images from the cross-section of PM2000 after DPD to a strain of (a) 1.0 and (b) 2.1. Regions framed in the images on the left-hand side are magnified on the right-hand side to demonstrate deformed particles in more detail. The compression axis is parallel to the scale bar.

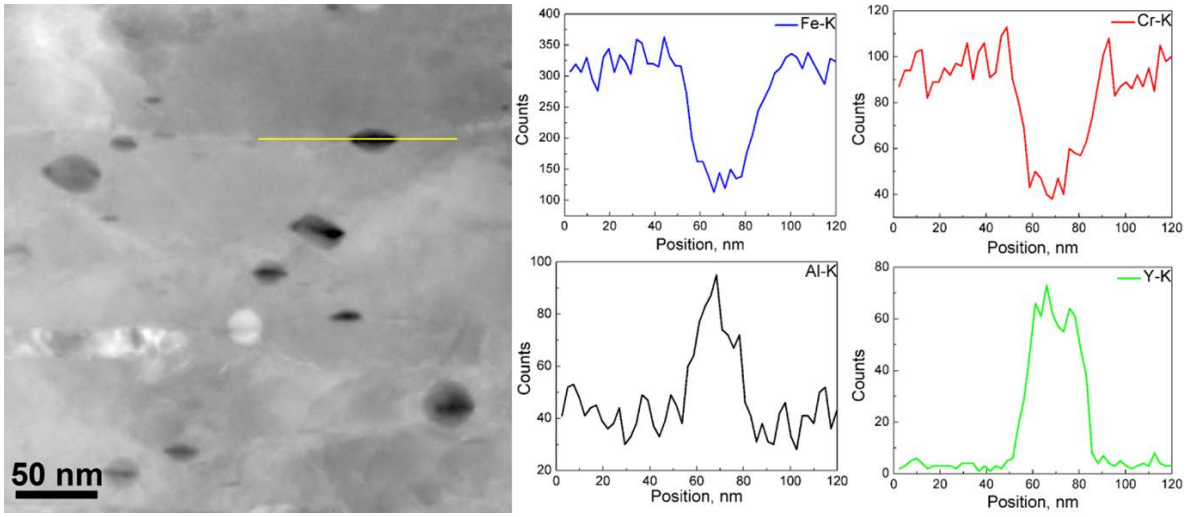

Fig. 4. A STEM image of PM2000 after DPD to a strain of 2.1. The EDX spectra on the right side correspond to the line scanning result in the STEM image.

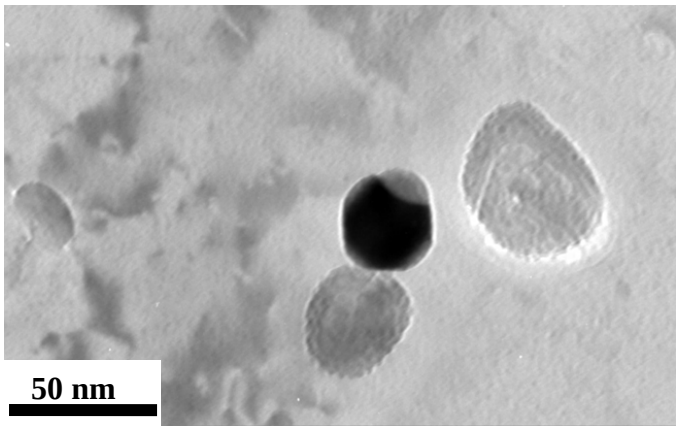

Fig.5. A TEM image showing deformed particles in the compression plane of PM2000 after DPD to a strain of 2.1.

3.3 Analysis of deformed oxide particles. The aspect ratio (AR) characterizing the shape of oxide nanoparticles in the cross-section can be used to evaluate the plastic strain experienced by these particles during DPD. Statistical data illustrating the relationship between the particle size calculated as the equivalent circular diameter (ECD) and AR after DPD to strains of 1.0 and 2.1 are shown in Fig. 6. This figure reveals three important findings: (i) the AR of oxide nanoparticles increases with macroscopic strain; (ii) the AR tends to increase with decreasing particle size; and (iii) most ECDs of the deformed particles are less than 15 nm. The latter results can further be validated by comparing frequencies of particles with ECD below 15 nm in the as-received and DPD samples. Assuming that undeformed particles in the strain 2.1 sample are characterized by an aspect ratio below 1.2, the percentage of such particles after DPD is 12%, which is substantially smaller than the frequency of such non-elongated particles of this size in the as-received condition, 74%.

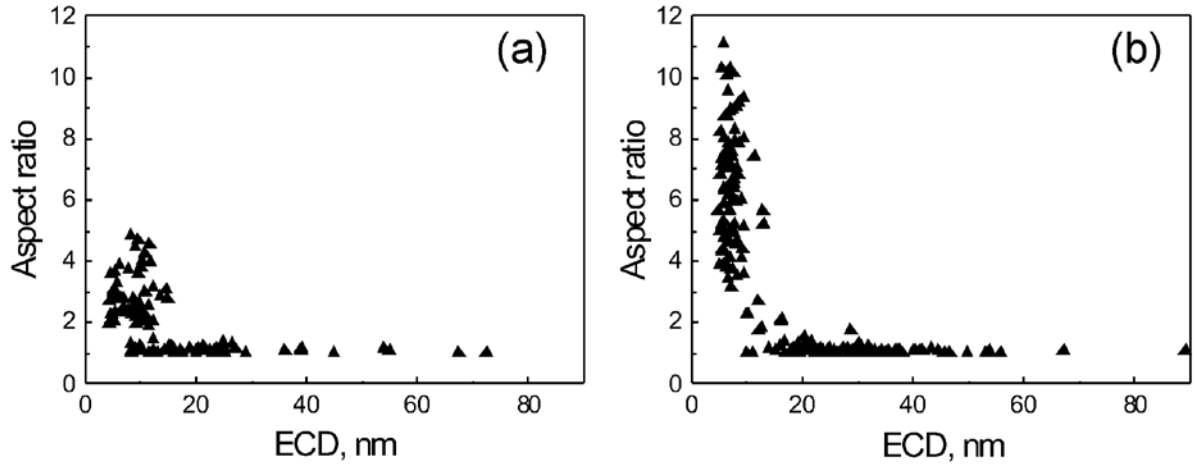

Fig. 6. Characteristics of oxide nanoparticles after DPD to strains of 1.0 (a) and 2.1 (b).

Considering that the oxide nanoparticles had a nearly spherical shape before DPD, the true plastic strain of particles after deformation can be estimated from their aspect ratio as $\varepsilon_{part} = 2\ln AR/3$. The plastic strain calculated using this relation is shown in Fig. 7, which represents the data only for particles with AR > 1.2, i.e. for the deformed particles. The mean value of true plastic strain for the oxide nanoparticles is 0.7 and 1.2 for the samples DPD-processed to strains of 1.0 and 2.1, respectively. Thus, the particle strain is substantially smaller than the macroscopic strain.

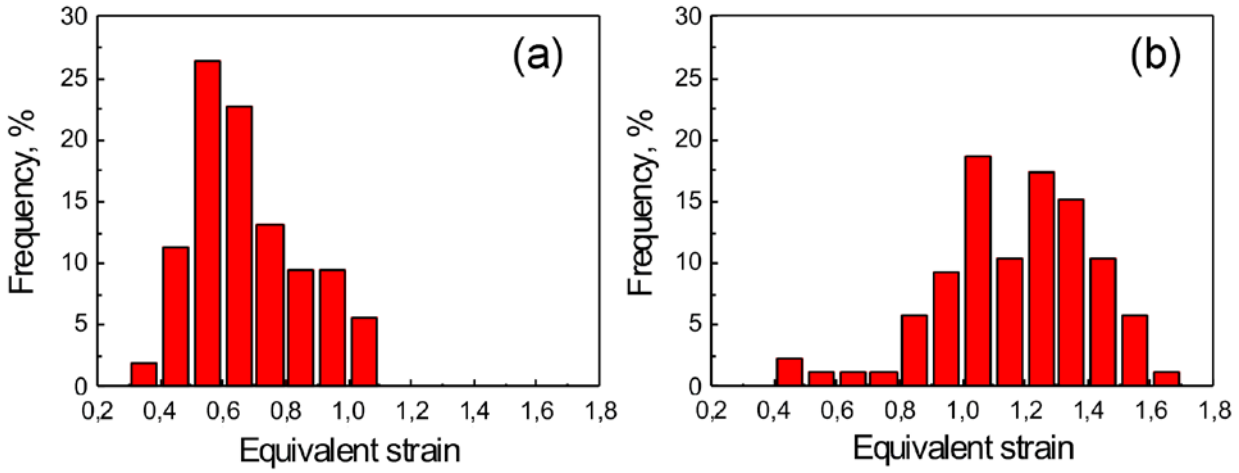

Fig. 7. Frequencies of particles (with aspect ratios above 1.2) deformed by DPD to equivalent strains of (a) 1.0 and (b) 2.1.

4. DISCUSSION

In the present experiment, oxide nanoparticles are found to undergo substantial plastic deformation during DPD of ODS steel, which may have important implications for better understanding the strengthening mechanisms in ODS steels. The strain experienced by particles (estimated from their shape change) increases with increasing macroscopic strain, remaining always smaller than the imposed macroscopic strain. It is pertinent to mention that for spherical particles subjected to compression to strains of 1.0 and 2.1, the aspect ratio $AR = \exp(3\varepsilon/2)$ is expected to 4.5 and 23.3, respectively. Apparently, the values obtained in the present experiment, 0.7 and 1.2, are much smaller than the predicted values.

According to Baker, Gove and Charles (1976), during deformation of steels containing non-metallic inclusions, significant stresses are exerted on particles by the matrix, which tends to force them deform in a manner similar to that of the matrix. Particles are considered to be deformed by forces at the particle/matrix interface. The extent of particle deformation depends primarily on the ratio of the flow stress between deformable particles and the matrix. Having summarized a number of particle/matrix systems, Gove and Charles (1974) proposed that the ratio between the true plastic strain of the particles and the true plastic strain of the matrix $\varepsilon_{part}/\varepsilon_{matr} \cong 2 - H_{part}/H_{matr}$ is controlled by the hardness H_{part} and H_{matr} of particles and matrix, respectively. As follows from this relationship, a particle will undergo little or no deformation if it is more than twice harder than the matrix. The Vickers hardness of bulk $YAlO_3$ is reported to be approximately 2000 HV (Weber, Bass, Andringa, Monchamp and Comperch 1969), while the measured Vickers hardness of the as-received PM2000 is only about 310 HV. If all oxide particles in our material had the same hardness as the bulk $YAlO_3$ sample tested by Weber et al. (1969), the oxide particles could hardly be deformed in the considerably softer ferritic matrix. Our experiment indicates, however, that particles of different sizes deform differently, i.e. that particles with ECDs larger than 20 nm are not appreciably deformed during DPD, whereas the majority of the smaller particles change their shape and aspect ratio (see Fig. 6). Since a reduction in particle size is expected to even reduce the energy available for deformation of the particles (Baker et al. 1976), the observed size dependence of the particle deformation behavior cannot be explained by different stresses exerted on particles of different sizes. Therefore, it is suggested that in our material small oxide particles are either intrinsically softer than coarser ones or the interface between particles and matrix depends on the particle size and thus can exert higher forces on smaller particles. Further work is required to establish whether the observed

size dependence is due to the very high strain rates applied during DPD or whether it holds at different strain rates.

5. SUMMARY

The microstructure and the behavior of oxide nanoparticles have been characterized in the ferritic ODS steel PM2000 compressed by DPD to different strains. A dislocation cell structure formed after deformation to a strain of 1.0 is found to evolve into nanoscale lamellae with an average lamellar spacing of about 70 nm after a strain of 2.1. The microstructure contains nanoparticles identified by HRTEM as yttrium aluminum perovskite $YAlO_3$. Furthermore, TEM and STEM-EDX analysis indicate that during DPD oxide nanoparticles with a size of less than 15 nm change their shape and aspect ratio, whereas particles coarser than 20 nm remain stable. The observed size dependence implies that the small oxide particles in our material are intrinsically easier to be deformed than coarser ones.

ACKNOWLEDGEMENTS

Financial support from the Sino-Danish Center for Education and Research is gratefully acknowledged. The authors are grateful to Prof. M. Heilmaier for providing the initial PM2000 sample. OVM also gratefully acknowledges the support from the Danish National Research Foundation (Grant No. DNRF86-5) and the National Natural Science Foundation of China (Grant No. 51261130091) to the Danish-Chinese Center for Nanometals.

REFERENCES

Baker, T.J., Gove, K.B. and Charles, J.A. (1976). Inclusion deformation and toughness anisotropy in hot-rolled steels. Metals Technol. 198, 183−193.

Chant, I. and Murty, K.L. (2010). Structural materials issues for the next generation fission reactors. JOM 62, 67−74.

Gove, K. B. and Charles, J., A. (1974). Further aspects of inclusion deformation. Metals Technol. 156, 425−431.

Hirata, A., Fujita, T., Wen, Y. R., Schneibel, J.H., Liu, C.T. and Chen, M.W. (2011). Atomic structure of nanoclusters in oxide-dispersion-strengthened steels. Nature Mater. 10, 922−926.

Hsiung, L.L., Fluss, M.J., Tumey, S.J., Choi, B.W., Serruys, Y., Willaime, F. and Kimura, A. (2010). Formation mechanism and the role of nanoparticles in Fe-Cr ODS steels developed for radiation tolerance. Phys. Rev. B 82. 184103-1−184103-13.

Krautwasser, P., Czyrska-Filemonowicz, A., Widera, M. and Carsughi, F. (1994). Thermal stability of dispersoids in ferritic oxide-dispersion-strengthened alloys. Mater. Sci. Eng. A 177, 199−208.

Li, Y.S., Tao, N.R. and Lu, K. (2008). Microstructural evolution and nanostructure formation in copper during dynamic plastic deformation. Acta Mater. 56, 230−241.

Miller, M.K., Hoelzer, D.T., Kenik, E.A. and Russell, K.F. (2005). Stability of ferritic MA/ODS alloys at high temperatures. Intermetallics 13, 387−392.

Odette, G.R., Alinger, M.J. and Wirth, B.D. (2008). Recent developments in irradiation-resistant steels. Ann. Rev. Mater. Res. 38, 471−503.

Ribis, J. and de Carlan, Y. (2012). Interfacial strained structure and orientation relationships of the nanosized oxide particles deduced from elasticity-driven morphology in oxide dispersion strengthened materials. Acta Mater. 60, 238−252.

Weber, M.J., Bass, M., Andringa, K., Monchamp, R.R. and Comperch, E. (1969). Czochralski growth and properties of $YAlO_3$ laser crystals. Appl. Phys. Lett. 15, 342−344.